Femtochemistry and Femtobiology
M.M. Martin and J.T. Hynes (editors)

Ultrafast scattering of electrons in TiO_2

M. Bonn[a], F. Wang[b], J. Shan[b], T.F. Heinz[b] and E. Hendry[a]

[a] Leiden Institute of Chemistry, Leiden University, P.O. Box 9502, 2300 RA Leiden, The Netherlands. e-mail: m.bonn@chem.leidenuniv.nl

[b] Departments of Physics and Electrical Engineering, Columbia University, 538 West 120th St., New York, NY 10027

ABSTRACT

Titanium dioxide (TiO_2) is widely used in photocatalysts and solar energy converters. A key factor determining the efficiency of these devices is the transport of photogenerated electrons. Electron mobility is determined by the scattering rate – the average frequency of momentum-changing collisions, inversely proportional to the electron mean free path. We elucidate the nature and rate of electron scattering in single-crystal rutile TiO_2 using the contact-free technique of THz time-domain spectroscopy. Strong electron-phonon interactions result in the formation of polarons, electrons dressed by local lattice deformations, and electron-phonon scattering rates up to 10^{14} s^{-1} at room temperature. The anomalous high scattering rates result in a low room temperature electron mobility of ~0.5 cm^2/Vs, which sets the intrinsic limit for device performance.

1. INTRODUCTION

In photo-catalytic and solar energy conversion devices, the absorption of a photon results in the generation of electrons and holes, which, upon separation, can provide an electric potential or trigger chemistry. The efficiency of these devices is frequently determined by the transport of the charges following photo-generation. In particular, for TiO_2-based dye-sensitized solar cells, it has been demonstrated that the efficiency is limited by electron transport through TiO_2 nanoparticles [1].

Although the transport of electrons in TiO_2 has consequently received considerable attention, several aspects of charge transport in TiO_2 remain ambiguous: Reported room-temperature electron Hall mobilities range from 0.01 to 10 cm^2/Vs [2]. In addition, the precise nature of the transport has remained unresolved. It is clear that the ionic character of the lattice combined with the presence of an electron in the conduction band (following optical excitation) results in a local deformation of the TiO_2 lattice, as the electron attracts positive Ti and repels negative O species (see inset in Fig. 1). This electron-phonon coupling effects the formation of a polaron [3], a quasi-particle consisting of an electron and the accompanying lattice deformation. The character of polarons in TiO_2 has remained unclear. In the limit of sufficiently strong coupling, s*mall* polarons are formed. These polarons display self-trapping of the electron and localized wavefunctions, with charge transport typically occurring through tunnelling or thermally activated hopping. For weaker coupling, *large* polarons appear, with

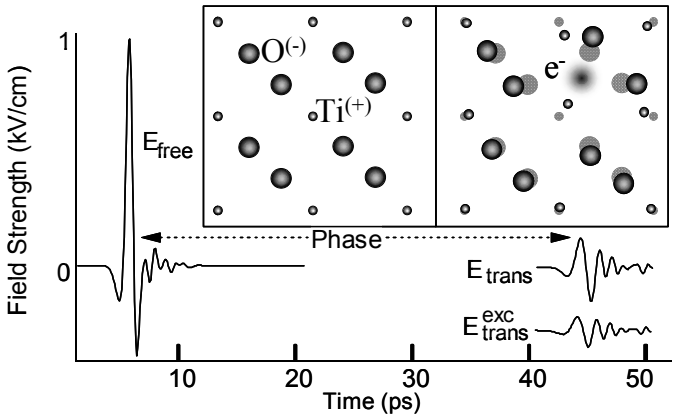

Fig. 1. Three THz-scans at 10K: The pulse transmitted through air ($E_{free}(t)$), the unexcited sample ($E_{trans}(t)$), and the photoexcited sample ($E^{exc}_{trans}(t)$). The 45ps delay between E_{free} and E_{trans} is caused by the large real part of the dielectric function (see inset of Fig. 2). A less obvious phase shift also exists between E_{trans} and E^{exc}_{trans} associated with the real part of $\Delta\varepsilon$. Inset: Left – the (001) face of rutile. Right – the lattice distortion when an electron is placed in the polar lattice results in polaron formation: (partly) positively charged Ti-atoms are attracted, and (partly) negative O-atoms repelled (see text).

spatially extended wavefunctions and band-type conduction. In both cases, the moving electron entrains the lattice deformation, resulting in an effective mass exceeding its band mass. There have been conflicting arguments for the existence of small and large polarons in rutile. We circumvent previous experimental limitations by investigating electron transport in defect-free (stoichiometric) single-crystal rutile TiO_2 using the method of contact-free terahertz time-domain spectroscopy (THz-TDS) [4] following photogeneration of electrons. We determine temperature dependent scattering rates from which the mobility, effective mass and polaron size can be inferred by means of the Feynman polaron model.

2. EXPERIMENTAL

The TiO_2 samples, mounted in a helium cryostat (10-300 K), are 1mm-thick (001) and (110)-cut single crystals to study the electronic response with the (THz) electric field perpendicular ($\perp$) and parallel (//) to the **c** axis, respectively. Rutile is the most common and stable TiO_2 polymorph and has a tetragonal structure with a=4.6Å and c=2.9Å. The band gap of rutile is 2.9 eV at room temperature, increasing slightly at lower temperatures.

The transport of electrons in TiO_2 is investigated with an experimental set up similar to that described in Ref. [4]. Electrons are excited into the conduction band through photo-excitation by 400 and 800 nm pulses of ~120 fs duration at excitation fluences of 4 J/m^2 and 30 J/m^2, respectively. The same Ti:Sa laser source is used to generate THz pulses [4]. As shown in Fig. 1, THz pulses are essentially single cycle electromagnetic pulses, the field strength $E(t)$ of which is detected directly in the time domain. The THz pulses are generated and detected through optical rectification and electro-optic sampling, respectively, of 800 nm pulses in ZnTe crystals. The ~1 ps cycle time corresponds to a frequency of 1 THz, and the shortness of the pulse (also ~1 ps) implies a large frequency bandwidth. Fig. 1 depicts the transmission of these pulses through air ($E_{free}(t)$), through the unexcited sample ($E_{trans}(t)$), as well as through the irradiated sample ($E^{exc}_{trans}(t)$) in which electrons have been excited into the conduction band [5]. Data analysis is most conveniently performed in the frequency domain,

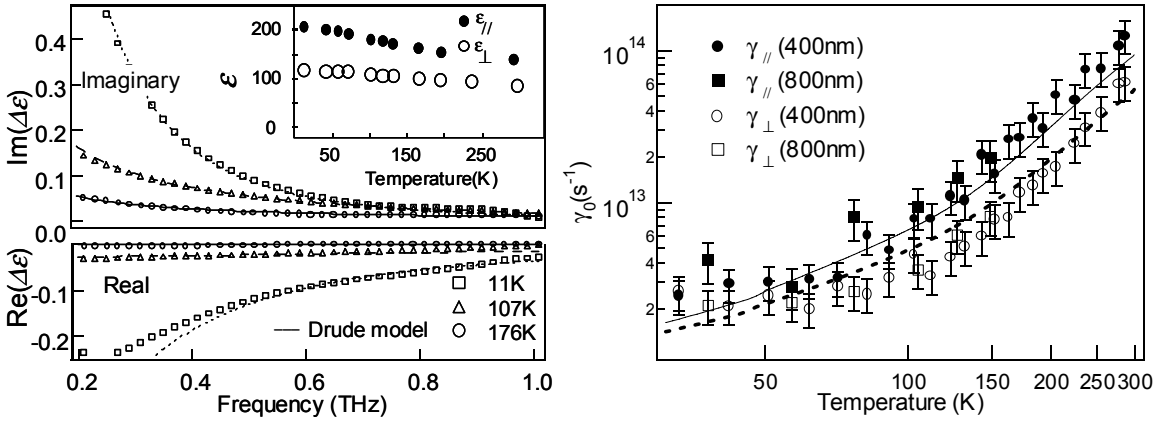

Fig. 2. (left) and 3. (right): Observed change in complex refractive index due to electron generation in TiO_2 with 400nm laser pulses at 11K, 107K and 176K. The Drude model describes the data very well, with varying scattering rates (see Fig. 3, right). Inset: the unperturbed dielectric function at 0.6THz measured at different temperatures. Right: Scattering rates $\gamma_{//}$ (closed symbols, parallel to the **c** axis) and $\gamma_{\perp}$(open symbols, perpendicular to the **c** axis), obtained with 400 and 800 nm excitation (circles and boxes, resp.). The lines are the result of the Feynman polaron model, with $\alpha_{//}$=4 (full line) and $\alpha_{\perp}$=6 (dashed line).

and the Fourier transforms of the first two measurements ($E_{free}(\omega)$ and $E_{trans}(\omega)$) yield the complex dielectric function $\varepsilon(\omega)$ of TiO_2 in the frequency range 0.2—1.0 THz. More interestingly, from $E_{trans}(\omega)$ and $E^{exc}_{trans}(\omega)$, we can obtain the change in $\varepsilon(\omega), \Delta\varepsilon(\omega)$, due to the presence of electrons in the conduction band. Whereas $\varepsilon(\omega)$ is determined by the response of the TiO_2 lattice, $\Delta\varepsilon(\omega)$ contains information on electron transport. Note that we can obtain both the real and imaginary parts of the dielectric functions, $\varepsilon(\omega)$ and $\Delta\varepsilon(\omega)$ from the direct characterization of the time-domain electric field provided by THz TDS.[4]

3. RESULTS AND DISCUSSION

For unexcited rutile, the real part of $\varepsilon(\omega)$, as derived from $E_{free}(\omega)$ and $E_{trans}(\omega)$, is observed to be very large, $\mathrm{Re}(\varepsilon) \approx 150$, with considerable anisotropy between directions parallel and perpendicular to the crystallographic **c** axis, and a magnitude decreasing slightly with increasing temperature (see inset of Fig. 2). $\Delta\varepsilon(\omega)$ – the pump induced change in dielectric function obtained from $E_{trans}(\omega)$ and $E^{exc}_{trans}(\omega)$ [6] – is shown in Fig. 2 for three different sample temperatures. The shape of these curves reflects the nature of the transport process. We fit the results using the simple Drude model for charge carrier transport: $\Delta\varepsilon(\omega) = -\omega_p^2/\left(\omega^2 + i\omega\gamma_o\right)$. Here γ_o denotes the scattering rate, which is the critical parameter describing charge transport, since it determines the mean time between momentum changing collisions that act to impede the flow of current. The plasma frequency ω_p is given by the electron (polaron) effective mass (m^{**}), the density of electrons (n_f), and the permittivity of free space (ε_0) through $\omega_p^2=(4\pi e^2 n_f)/(\varepsilon_0 m^{**})$. By modeling the data using this functional form, we are able to extract γ_o and ω_p, the two key parameters determining the electrical conductivity of TiO_2. At high temperatures, the scattering rate cannot be found by a direct fitting procedure, but can be inferred directly from the amplitude of the induced THz signal.

As shown in Fig. 3, there is a sharp rise in γ_o with increasing temperature. The anisotropy of electron transport is also clearly evident, with a larger scattering rate measured along parallel direction. The large scattering rates at room temperature ($\gamma_o \approx 100$ THz) are a consequence of the strong electron-phonon coupling and the increased phonon density at elevated temperatures.

At low temperatures, scattering from low-frequency *acoustic* phonons dominates, with a $T^{3/2}$ temperature dependence [7]. As the temperature is increased, excitation of higher frequency *optical* phonons occurs, leading to enhanced scattering. The LO phonon mode from which scattering prevails can be inferred from the frequency dependent dielectric function (ε) obtained from infrared reflectance data. It is found to be two different 800 cm^{-1} phonon modes for the two crystallographic directions. The concomitant electron-phonon coupling constant α can be obtained from a fit to our temperature dependent scattering data, using the polaron theory of Feynman [8]. The results of the fit are shown in Fig. 3, with $\alpha_{//}=4$ and $\alpha_{\perp}=6$ the electron-phonon coupling constant parallel and perpendicular to the crystal c-axis, respectively. The strong electron-phonon coupling, also evident from the large static dielectric function (inset in Fig. 2,) results in mobilities of $\mu_{//}=0.6$ cm^2/Vs and $\mu_{\perp}=0.2$ cm^2/Vs for parallel and perpendicular directions respectively.

The resulting polaron radius of $r_{pol} \sim 5$ Å is substantially smaller than the ~25 nm radius of particles typically used in devices such as solar cells. Therefore, quantum confinement effects are expected to be negligible. Further, the large scattering rates (and correspondingly short mean free paths, also ~5 Å) imply that momentum relaxation of polarons at room temperature is be dominated by the bulk properties of TiO_2 and that the surface scattering effects that have been observed at low temperatures (77 K) [9] are of minor significance at room temperature. The much lower room-temperature drift mobility of photogenerated polarons reported for *porous* rutile TiO_2 ($<10^{-3}$ cm^2/Vs, as opposed to ~0.5 cm^2/Vs reported here) indicates the existence of a barrier for motion between the structures. This might arise either from surface traps or from barriers encountered by electrons entering or leaving individual particles. Our results show that, although electron transport through bulk TiO_2 is impeded by scattering associated with the strong electron-phonon interaction, it is not the bulk mobility that limits transport. The mobility (~0.5 cm^2/Vs) observed here represents the intrinsic limit for electron transport at room temperature and suggests that substantial device improvement is possible for optimized nanoparticle composites.

REFERENCES

[1] N. Kopidakis, et al., J. Phys. Chem. B 104 (2000) 3930.

[2] R. G. Beckenridge and W. R. Hosler, Phys. Rev. 91 (1953) 793; E. Yagi, R. R. Hasiguti, and M. Aono, Phys. Rev. B 54 (1996) 7945.

[3] N. M. A. S. Alexandrov, Polarons and Bipolarons (World Scientific, Singapore, 1995), 1st Ed., pp. 155-157.

[4] M. C. Beard, G. M. Turner, and C. A. Schmuttenmaer, J. Phys. Chem. B 106 (2002) 7146.

[5] By comparing experiments on photo-excited TiO_2 to n-type doped TiO_{2-x},(x=0.0005) we conclude that the pump-induced THz absorption originates primarily from photo-generated electrons, rather than from holes, in accordance with the large hole band mass ($>4m_e$).

[6] E. Knoesel, M. Bonn, J. Shan, et al., Phys. Rev. Lett. 86 (2001) 340.

[7] J. Bardeen and W. Shockley, Phys. Rev. 80 (1950) 72.

[8] R. P. Feynman, Phys. Rev. 97 (1955) 660; R. P. Feynman., *ibid.* 127 (1962) 1004.

[9] G. M. Turner, M. C. Beard, and C. A. Schmuttenmaer, J. Phys. Chem. B 106 (2002) 11716.